

Comparison of ^{18}F -fluoromethylcholine and 2-deoxy-D-glucose in the distribution of tumor and inflammation

Kazuo KUBOTA,* Shozo FURUMOTO,** Ren IWATA,** Hiroshi FUKUDA,***
Kazunori KAWAMURA**** and Kiichi ISHIWATA****

*Division of Nuclear Medicine, Department of Radiology, International Medical Center of Japan

**Cyclotron and Radioisotope Center, Tohoku University

***Institute for Development, Aging and Cancer, Tohoku University

****Tokyo Metropolitan Institute for Gerontology

Purpose: The distribution characteristics of ^{18}F -fluoromethylcholine (^{18}F -choline) in tumor and inflammatory tissue were compared with those of ^{14}C or ^3H -2-deoxyglucose (2DG) as a substitute for fluorodeoxyglucose (FDG). **Methods:** A solid tumor model of AH109A in the back of Donryu rats and an aseptic inflammation model of turpentine oil injection subcutaneously in rats were used for experiments. Tissue distribution was examined at 5, 30 and 60 min after injection of a mixture of ^{18}F -choline and ^3H -2DG. Double-tracer high-resolution autoradiographs (ARGs) of tumor and inflammation were obtained using ^{18}F -choline and ^{14}C -2DG. Whole body (WB) ARG was performed with ^{18}F -choline. **Results:** Tumor uptake of ^{18}F -choline reached a peak at 30 min, when the tumor to blood ratio was 5.1. Both tumor and inflammation uptake of 2DG were higher than those of ^{18}F -choline. ^{18}F -choline uptake by inflammation was lower than that by tumor. The tumor to brain uptake ratio was 5.7 with ^{18}F -choline and 1.2 with 2DG. In the ARG of inflammation, linear or ring-like structures of 2DG uptake were observed in the wall of the abscess, but were not identified with ^{18}F -choline. Photomicrography showed that the uptake was limited to granulocytes, macrophages and fibroblasts, consistent with sub-acute or chronic inflammation. **Conclusion:** ^{18}F -choline uptake by inflammation was lower than that of 2DG in the tissue distribution study, and ^{18}F -choline uptake by abscess wall was significantly lower than that of 2DG in the autoradiography study. Our results may suggest the feasibility of ^{18}F -choline-PET imaging for the differential diagnosis of cancer and chronic inflammation in lung and brain.

Key words: ^{18}F -fluorocholine, 2-deoxyglucose, inflammation, tumor, autoradiography

INTRODUCTION

POSITRON EMISSION TOMOGRAPHY (PET) using ^{18}F -fluorodeoxyglucose (FDG) has been used widely, and its excellent diagnostic ability for a wide variety of tumors has been established. However, FDG-PET has several disadvantages, such as high urinary excretion rates interfering with tumor detection in the pelvis, low uptake by

several types of tumors, high uptake by inflammation, and high physiological brain uptake lowering tumor to background contrast. In order to compensate for these disadvantages, ^{11}C -methionine, ^{11}C -choline and other tracers have been developed and evaluated. ^{11}C -choline has been developed by T. Hara and its efficacy for tumor imaging has now been evaluated in brain,¹ prostate,² bladder,³ gynecological,⁴ lung,⁵ esophageal⁶ and head and neck⁷ cancers. Because of its low urinary excretion rate, ^{11}C -choline has a unique advantage in imaging of prostate cancer.⁸ Low physiological uptake of ^{11}C -choline by the brain facilitates the delineation of brain tumors.⁹ In thoracic tumors, low uptake by inflammation has also been suggested.¹⁰

In order to overcome the limited utility of the

Received April 26, 2006, revision accepted July 19, 2006.

For reprint contact: Kazuo Kubota, M.D., Ph.D., Division of Nuclear Medicine, Department of Radiology, International Medical Center of Japan, 1-21-1 Toyama, Shinjuku-ku, Tokyo 162-8655, JAPAN.

E-mail: kkubota@imcj.hosp.go.jp

Table 1 Double tracer tissue distribution study using AH109A tumor and inflammation model of rats*

¹⁸ F-choline	5 min (n = 3)		30 min (n = 7)		60 min (n = 7)	
Tissue	mean ± SD	T./Or.**	mean ± SD	T./Or.	mean ± SD	T./Or.
Blood	0.109 ± 0.018	1.092	0.055 ± 0.008	5.145	0.042 ± 0.005	6.262
Muscle	0.351 ± 0.043	0.339	0.326 ± 0.06	0.868	0.343 ± 0.026	0.767
Liver	0.985 ± 0.07	0.121	1.24 ± 0.251	0.228	1.08 ± 0.192	0.244
Intestine	0.739 ± 0.12	0.161	0.907 ± 0.177	0.312	0.874 ± 0.172	0.301
Myocardium	0.519 ± 0.077	0.229	0.554 ± 0.068	0.511	0.583 ± 0.047	0.451
Kidney	3.628 ± 0.427	0.033	3.856 ± 0.488	0.073	3.46 ± 0.484	0.076
Brain	0.058 ± 0.013	2.052	0.05 ± 0.011	5.66	0.048 ± 0.007	5.479
Tumor	0.119 ± 0.036	1	0.283 ± 0.047	1	0.263 ± 0.067	1
Inflammation	0.174 ± 0.02	0.684	0.189 ± 0.019	1.497	0.193 ± 0.013	1.363
Bone	0.311 ± 0.043	0.383	0.421 ± 0.032	0.672	0.539 ± 0.041	0.488

³ H-2DG	5 min (n = 3)		30 min (n = 7)		60 min (n = 7)	
Blood	1.955 ± 1.837	0.359	0.204 ± 0.056	9.108	0.216 ± 0.231	8.681
Muscle	0.169 ± 0.014	4.243	0.183 ± 0.124	10.153	0.176 ± 0.089	10.653
Liver	0.6 ± 0.054	1.195	0.205 ± 0.034	9.063	0.163 ± 0.036	11.503
Intestine	0.468 ± 0.062	1.532	0.464 ± 0.108	4.004	0.519 ± 0.076	3.613
Myocardium	0.239 ± 0.032	3.0	0.158 ± 0.024	11.759	0.164 ± 0.048	11.433
Kidney	1.152 ± 0.172	0.622	0.434 ± 0.184	4.281	0.252 ± 0.057	7.44
Brain	1.087 ± 0.084	0.66	1.489 ± 0.165	1.248	1.434 ± 0.109	1.308
Tumor	0.717 ± 0.187	1	1.858 ± 0.369	1	1.875 ± 0.405	1
Inflammation	0.455 ± 0.063	1.576	0.595 ± 0.159	3.123	0.635 ± 0.084	2.953

* % Inj/g; Percentage of the tissue radioactivity per gram against the injected radioactivity.

** Tumor/Organ ratio

Table 2 Distribution of ¹⁸F-choline and 2DG in inflammation by double tracer ARG (Grain density)

Lesions (n = 6)	¹⁸ F-choline	¹⁴ C-2DG	P value*
Abscess wall	62.7 ± 14.3	109.4 ± 7.1	p < 0.0001
Abscess center	33.0 ± 6.2	30.6 ± 5.1	not significant

Data are mean ± SD.

*Statistical analysis by Student's t-test.

carbon-11 tracer due to its short half-life, fluorine-18-labeled choline analogues have been developed. ¹⁸F-fluoromethylcholine¹¹ appears to more closely resemble its original compound ¹¹C-choline than does ¹⁸F-fluoroethylcholine,¹² due to the lower urinary excretion and lower metabolic degradation. However, the distribution characteristics of ¹⁸F-fluoromethylcholine in tumor and inflammation tissue have not yet been thoroughly evaluated. Here, we compared the distribution patterns of ¹⁸F-fluoromethylcholine with ¹⁴C/³H-2-deoxyglucose as a substitute for FDG, in inflammation and tumor models, using high resolution double tracer autoradiography and a double-tracer tissue distribution study.

MATERIALS AND METHODS

Animals and study protocol

Rat AH109A tumor (undifferentiated hepatoma, developed and stocked in Tohoku University) was in-

oculated subcutaneously (s.c.) into the back of 6- to 7-week-old male Donryu rats (body weight 265 ± 17 g, mean ± SD). Turpentine oil (0.3 ml) was also inoculated s.c. into the back of the same rats to produce an aseptic inflammation model as reported previously.¹³ Tissue distribution experiments and autoradiography experiments were performed 8 days after inoculation of AH109A, when the tumor size was about 1 cm in diameter, which was 4 days after inoculation of turpentine when the FDG uptake had peaked in our previous study.¹³

¹⁸F-fluoromethylcholine (¹⁸F-choline) was synthesized using the [¹⁸F]fluoromethyl triflate ([¹⁸F]CH₂FOTf) method as reported previously.¹⁴ Briefly, [¹⁸F]fluoromethyl bromide ([¹⁸F]CH₂BrF) was first prepared from CH₂Br₂ by conventional nucleophilic substitution reaction using no-carrier-added [¹⁸F]KF and Kryptofix®222. After purifying with four Sep-Pak® Plus silica cartridges connected in series, [¹⁸F]CH₂BrF was converted to [¹⁸F]CH₂FOTf by passing it through a heated AgOTf column, and then [¹⁸F]CH₂FOTf was applied to solid-supported [¹⁸F]fluoromethylation of *N,N*-dimethylaminoethanol on a Sep-Pak® Plus C18 cartridge to produce ¹⁸F-choline. Subsequent purification of the product using an Accell CM cartridge according to a published procedure¹⁵ produced a final saline solution of ¹⁸F-choline with a radiochemical purity greater than 95%.

2-Deoxy-D-[1-¹⁴C]glucose (¹⁴C-2DG) with specific activity of 2.18 GBq/mmol and 2-[6-³H]deoxy-D-glucose (³H-2DG) with specific activity of 1.48 TBq/mmol were

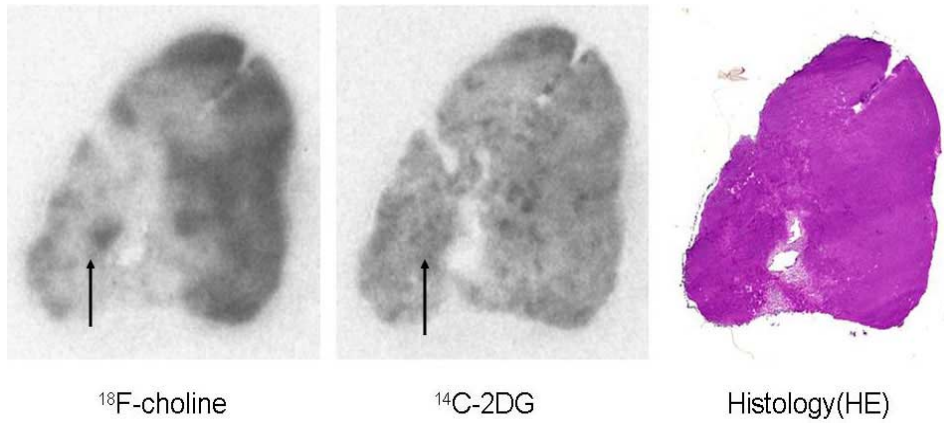


Fig. 1 Typical image of the same rat AH109A tumor with double-tracer ARG. *Left:* ^{18}F -choline, *middle:* ^{14}C -2DG, *right:* histology using HE staining. Note that the two hot spots on the ^{18}F -choline image (*arrows*) are not remarkable on the ^{14}C -2DG image, suggesting a slightly different distribution.

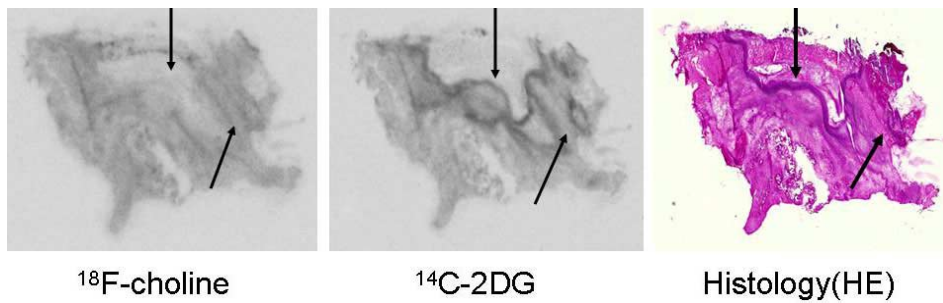


Fig. 2 A typical ARG image of the turpentine oil inflammation model, *left:* ^{18}F -choline, *middle:* ^{14}C -2DG, *right:* histology of HE-stained section. The linear or ring-like structures on ^{14}C -2DG images (*arrows*) are not seen in the ^{18}F -choline images.

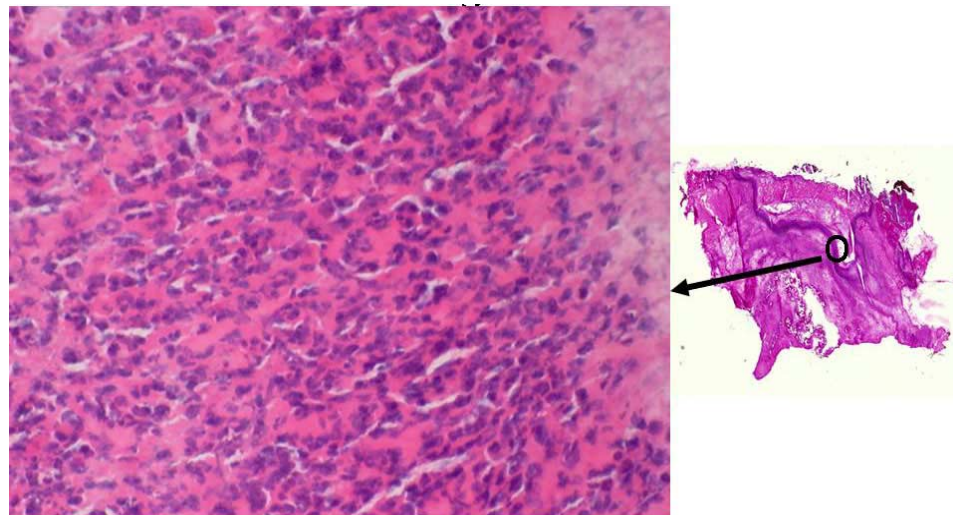


Fig. 3 Photomicrograph of the linear structure on the ^{14}C -2DG image of inflammation. 400 \times magnification of the histology on HE stain in Figure 2a. Sub-acute inflammation comprising macrophages, granulocytes and fibroblasts.

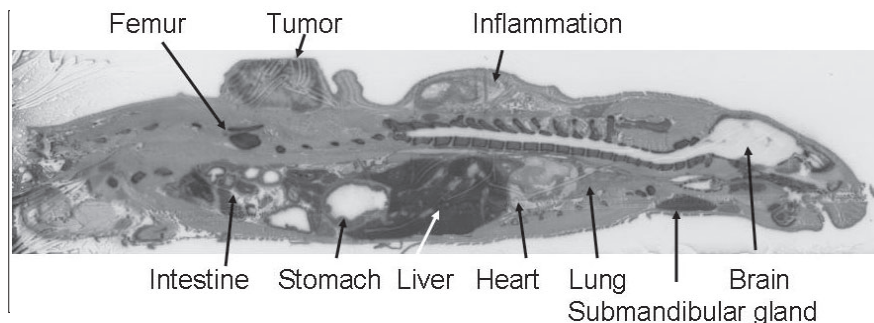


Fig. 4 Typical whole body autoradiography of the rat with tumor and inflammation using ^{18}F -choline. Note the high physiological uptake in abdominal organs, liver, intestine and kidney, and the lower uptake in the brain, lung and heart.

purchased commercially (American Radiolabeled Chemicals Inc.).

Tissue distribution

A mixture of 7.5 MBq of ^{18}F -choline and 370 kBq of ^3H -2DG was injected into the rats intravenously through the lateral tail vein. Five ($n = 3$), 30 ($n = 7$) or 60 ($n = 7$) minutes after injection, the rats were sacrificed with an overdose of chloroform anesthesia. Tissue and organ samples were dissected, blotted and weighed. Blood samples were obtained by heart puncture, tumor samples were obtained from the periphery of the tumor mass (avoiding necrosis), and a sample of inflammation was obtained from the wall of the abscess. ^{18}F radioactivity was measured just after the experiments using an automated gamma counter with decay correction. After the decay of ^{18}F radioactivity, about 0.1 g of tissue was bleached and dissolved into a scintillation cocktail. Radioactivity of ^3H was measured using a liquid scintillation counter. Tissue radioactivity per gram was expressed as the percentage of the injected dose (%Inj/g).

Autoradiography

One hundred and eighty-five MBq of ^{18}F -choline and 740 kBq of ^{14}C -2DG was injected i.v. in rats with tumor and inflammation ($n = 3$, each). One hour after injection of ^{14}C -2DG, 30 min after injection of ^{18}F -choline, the rats were sacrificed with an overdose of anesthesia. Samples of tumor or inflammation were dissected, trimmed, embedded in O.C.T. compound (Miles Inc.) and frozen with liquid nitrogen. The frozen sample blocks were sectioned on a cryostat at -25°C . The 10- μm -thick sections were mounted on clean glass slides, air-dried and placed in direct contact with autoradiography (ARG) films (BioMax MR, Kodak) in film cassettes for 4 hr to produce the ^{18}F -choline images. Two days after the initial ARG when the ^{18}F radioactivity had decayed, the same sections were placed in contact with other films for 10 days to produce the ^{14}C images. The slides were then fixed with alcohol and stained with hematoxylin and eosin to obtain the

histological images.

In order to obtain higher resolution of ARG images, ARG film was used instead of the phosphor computed imaging system (Fuji Film Co., Tokyo). The approximate resolution of ARG film was 3 μm and of phosphor imager 30 μm in full width half maximum (data not shown). The ARG images of inflammation were digitized, and the grain density was quantified as described previously.¹⁶ Briefly, four regions of interest placed around the inflammation were averaged as the background. After subtraction of the background, small regions of interest were placed on each lesion, and the grain density was recorded. We analyzed two separate sections per inflammatory lesion of three rats, a total of 6 images of 2DG and ^{18}F -choline. Mean and SD of the grain density of the abscess wall defined as the dark stained, high cellularity band, and the abscess center defined as low cellular, including residual injected oil, exudate and cell debris area surrounded by the abscess wall were compared in each tracer (Table 2).

For whole-body ARG, three rats were embedded in 3% carboxymethylcellulose, frozen with acetone dry-ice, and sectioned on a cryostat at -25°C . The 30- μm -thick sections were obtained on an adhesive tape, mounted on cardboard, air-dried and placed in direct contact with ARG films (BioMax MR, Kodak) in cassettes for 4 hr to produce the ^{18}F -choline images.

The experimental protocol was reviewed and approved in advance by the laboratory animal care and ethics committee of participating institutions.

Statistical analysis

All data were expressed as mean \pm SD. Differences between groups were examined for statistical significance using the Student's t-test. A p value less than 0.05 denoted the presence of a statistically significant difference.

RESULTS

Table 1 shows the results of the tissue distribution experiments. Tumor uptake of ^{18}F -choline reached a peak at 30 min, with a tumor to brain ratio of 5.7, and tumor to blood ratio of 5.1. ^{18}F -choline uptake by inflammation was lower than that by the tumor. Tumor uptake of 2DG was higher than that of ^{18}F -choline. Inflammation uptake of 2DG was higher than that of ^{18}F -choline. The tumor to brain uptake ratio was higher for ^{18}F -choline than 2DG, suggesting that ^{18}F -choline may be advantageous in imaging brain tumors. ^{18}F -choline showed high kidney uptake from 5 to 60 min. Detection of abdominal tumors with ^{18}F -choline might be disturbed by high physiological uptake by abdominal organs, including liver and kidneys. Bone uptake of ^{18}F suggested a mild level of de-fluorination of ^{18}F -choline *in vivo*.

In the double tracer ARGs of tumor, ^{18}F -choline and 2DG showed slightly different distribution patterns (Fig. 1). 2DG uptake seemed to be in viable cancer cells and in granulation tissue, consistent with our previous report.¹⁷ ^{18}F -choline was localized mainly in viable cancer cells and little in necrotic tissue. In inflammation, linear or ring-like structures of 2DG uptake were identified in the wall of the abscess, which were not evident with ^{18}F -choline (Fig. 2). Photomicrography showed these to be comprised of granulocytes, macrophages and fibroblasts, consistent with acute or sub-acute inflammation (Fig. 3).

Results of quantitative evaluation of digitized ARG images are shown in Table 2. Images of both ^{18}F -choline and ^{14}C -2DG showed the same grain density in the abscess center, where residual injected oil, exudate and cell debris were observed histologically. In the wall of the abscess comprised of granulocytes, macrophages and fibroblasts, the density of 2DG ARG was significantly higher than that of ^{18}F -choline (Fig. 2).

Whole body ARG with ^{18}F -choline showed low uptake in the brain and chest. High physiological uptake was observed mainly in the abdomen, liver, intestine and kidney (Fig. 4). Positive tumor to background contrast was observed in the lung and brain with ^{18}F -choline. The grain density ratios of tumor to lung and to brain in digitized ARGs were 2.1 ± 0.2 and 7.7 ± 0.6 ($n = 3$), respectively.

DISCUSSION

In this study, we have compared the tissue distribution characteristics of ^{18}F -choline and 2DG in tumor and inflammation models. ^{18}F -choline uptake by inflammation was lower than that of 2DG, which was clearly shown by ARGs in which the abscess walls were 2DG-positive and ^{18}F -choline-negative.

Recently, ^{18}F -choline uptake by inflammation has been reported by Wyss et al.,¹⁸ who showed high uptake of ^{18}F -choline by bacterial inflammation in rats with autoradiog-

raphy and PET imaging experiments. They reported the SUV of abscess wall by ^{18}F -choline ARG as 3.0–4.0 at 7 to 11 days after inoculation of *Staphylococcus aureus*, 10 min after injection of ^{18}F -choline, and concluded that ^{18}F -choline is avidly accumulated in inflammatory infiltrates. It is not clear why their data showed a higher uptake than that of our study. In part, the differences between the models may explain the different results. In our study, ^{18}F -choline uptake by inflammation at 60 min after i.v. injection was 0.19%Inj/g, which is equivalent to 0.50 in SUV. Our model is of aseptic inflammation induced by chemical stimulation with turpentine oil. FDG uptake peaked in this model at 4 days after inoculation when the lesion was in the sub-acute phase, when the inflammation comprised granulocytes, macrophages and fibroblasts, as reported previously.¹³ The model used by Wyss et al.¹⁸ was more aggressive, with a greater degree of inflammatory activity associated with pyogenic bacterial infection with necrosis. These differences in the level of inflammation may explain the different results. Our findings suggest that in moderate inflammation, ^{18}F -choline uptake seems to be lower than that of FDG.

In the clinical setting, drastic pyogenic inflammation is easily recognized because of symptoms such as fever and cough or pain, and with various signs of inflammation such as elevated white blood cell count and C-reactive protein. On the contrary, the differential diagnosis of cancer from chronic inflammation with moderate activity such as tuberculosis is more difficult, and has become an important clinical demand for PET imaging. From this perspective, our results obtained using an inflammation model of moderate activity may be more feasible for the clinical setting of PET, and may encourage further clinical evaluation of ^{18}F -choline-PET.

We have reported the different distribution patterns of FDG and methionine in tumor tissue using a micro-autoradiography technique.^{17,19} In addition to cancer cells, high FDG uptake was seen in activated macrophages, leucocytes and in young granulation tissue, cells and tissues comprising non-neoplastic components (stroma) of tumor tissue. Compared to FDG, methionine distribution in tumor tissue is more specific for viable cancer cells, and indeed tumor uptake of methionine is predominantly by viable cancer cells. Macrophages and granulation tissue exhibited lower uptake of methionine than of FDG. In our separate study, the intra-tumoral distribution of ^{18}F -choline and methionine was almost the same (data not shown), suggesting that ^{18}F -choline uptake might also be localized mainly in viable cancer cells. This is consistent with our finding that ^{18}F -choline uptake by inflammation was lower than that of FDG in the tissue distribution study, and with the finding that ^{18}F -choline uptake by the abscess wall was significantly lower than that of FDG in the autoradiography study.

Cancer cells are known to be associated with elevated activity of choline kinase resulting in an increase in the

level of phosphorylcholine.²⁰ DeGrado et al.¹¹ reported that ¹⁸F-choline underwent phosphorylation *in vitro* by choline kinase with a phosphorylation rate equivalent to that of native ¹¹C-choline. Roivainen et al.²¹ analyzed blood metabolites of ¹¹C-choline and reported that the major metabolite in both human and rat plasma was identified as ¹¹C-betaine, a product of choline oxidation and not phosphorylation. ¹⁸F-choline may share the elevated transport of ¹¹C-choline however, the actual metabolic fates of ¹⁸F-choline and ¹¹C-choline in tumor tissue are still unclear.

Pieterman et al.²² reported that FDG uptake by thoracic primary tumors was significantly higher than ¹¹C-choline uptake, and that ¹¹C-choline-PET was less accurate than FDG-PET due to the lower accumulation of ¹¹C-choline in malignant tissue. Hara et al.¹⁰ compared FDG-PET and ¹¹C-choline-PET in lung cancer and pulmonary tuberculosis and found that FDG uptake was higher than that of ¹¹C-choline in both lung cancer and tuberculosis. These findings may be consistent with our present results, where tumor uptake of ¹⁸F-choline was lower than that of FDG, suggesting the limitations of ¹⁸F-choline for general use in tumor imaging. The different distribution pattern of ¹⁸F-choline compared to FDG in inflammation as seen in our autoradiography study might be helpful for the differential diagnosis of chronic inflammation and tumor in the lung using PET. In addition, the low physiological uptake by brain using ¹⁸F-choline, may suggest the feasibility of brain tumor imaging with PET. ¹⁸F-choline may have advantages over FDG for these specific purposes. Further clinical studies are required with ¹⁸F-choline and PET to address these issues.

CONCLUSION

¹⁸F-choline uptake by inflammation was lower than that of FDG in the tissue distribution study, and ¹⁸F-choline uptake by abscess wall was significantly lower than that of FDG in the autoradiography study. Our findings support the feasibility of ¹⁸F-choline-PET imaging for the differential diagnosis of cancer and chronic inflammation.

ACKNOWLEDGMENTS

This study was supported by a Grant-in-Aid for Scientific Research No. 16390349 from Japan Society for the Promotion of Science. Part of this study was financially supported by the Budget for Nuclear Research of the Ministry of Education, Culture, Sports, Science and Technology, based on screening and counselling by the Atomic Energy Commission.

REFERENCES

1. Hara T, Kosaka N, Shinoura N, Kondo T. PET imaging of brain tumor with [methyl-¹¹C]choline. *J Nucl Med* 1997; 38: 842–847.

2. Hara T, Kosaka N, Kishi H. PET imaging of prostate cancer using carbon-11-choline. *J Nucl Med* 1998; 39: 990–995.
3. de Jong IJ, Pruim J, Elsinga PH, Jongen MM, Mensink HJ, Vaalburg W. Visualization of bladder cancer using ¹¹C-choline PET: first clinical experience. *Eur J Nucl Med* 2002; 29: 1283–1288.
4. Torizuka T, Kanno T, Futatsubashi M, Okada H, Yoshikawa E, Nakamura F, et al. Imaging of gynecologic tumors: comparison of ¹¹C-choline PET with ¹⁸F-FDG PET. *J Nucl Med* 2003; 44: 1051–1056.
5. Hara T, Inagaki K, Kosaka N, Morita T. Sensitive detection of mediastinal lymphnode metastasis of lung cancer with ¹¹C-choline PET. *J Nucl Med* 2000; 41: 1507–1513.
6. Kobori O, Kiriwara Y, Kosaka N, Hara T. Positron emission tomography of esophageal carcinoma using ¹¹C-choline and ¹⁸F-fluorodeoxyglucose. *Cancer* 1999; 86: 1638–1648.
7. Ninomiya H, Oriuchi N, Kahn N, Higuchi T, Endo K, Takahashi K, et al. Diagnosis of tumor in the nasal cavity and paranasal sinuses with [¹¹C]choline PET: comparative study with 2-[¹⁸F]fluoro-deoxy-D-glucose (FDG) PET. *Ann Nucl Med* 2004; 18: 29–34.
8. Fazio E, Picchio M, Messa C. Is ¹¹C-choline the most appropriate tracer for prostate cancer? *Eur J Nucl Med Mol Imaging* 2004; 31: 753–756.
9. Ohtani T, Kurihara H, Ishiuchi S, Saito N, Oriuchi N, Inoue T, et al. Brain tumor imaging with carbon-11 choline: comparison with FDG-PET and gadolinium-enhanced MR imaging. *Eur J Nucl Med* 2001; 28: 1664–1670.
10. Hara T, Kosaka N, Suzuki T, Kudo K, Niino H. Uptake rates of ¹⁸F-fluorodeoxyglucose and ¹¹C-choline in lung cancer and pulmonary tuberculosis, a positron emission tomography study. *Chest* 2003; 124: 893–901.
11. DeGrado TR, Baldwin SW, Wang S, Orr MD, Liao RP, Friedman HS, et al. Synthesis and evaluation of ¹⁸F-labeled choline analogs as oncologic PET tracers. *J Nucl Med* 2001; 42: 1805–1814.
12. Hara T, Kosaka N, Kishi H. Development of ¹⁸F-fluoroethylcholine for cancer imaging with PET: synthesis, biochemistry and prostate cancer imaging. *J Nucl Med* 2002; 43: 187–199.
13. Yamada S, Kubota K, Kubota R, Ido T, Tamahashi N. High accumulation of fluorine-18-fluorodeoxyglucose in turpentine-induced inflammatory tissue. *J Nucl Med* 1995; 36: 1301–1306.
14. Iwata R, Pascali C, Bogni A, Furumoto S, Terasaki K, Yanai K. [F-18]Fluoromethyl triflate, a novel and reactive [F-18]fluoromethylating agent: preparation and application to the on-column preparation of [F-18]fluorocholine. *Appl Radiat Isot* 2002; 57: 347–352.
15. Pascali C, Bogni A, Iwata R, Cambie M, Bombardieri E. [¹¹C]Methylation on a C18 Sep-Pak cartridge: a convenient way to produce [N-methyl-¹¹C]choline. *J Label Comput Radiopharm* 2000; 43: 195–203.
16. Kubota K, Tada M, Yamada S, Hori K, Saito S, Iwata R, et al. Comparison of the distribution of fluorine-18 fluoromisonidazole, deoxyglucose and methionine in tumor tissue. *Eur J Nucl Med* 1999; 26: 750–757.
17. Kubota R, Yamada S, Kubota K, Ishiwata K, Tamahashi N, Ido T. Intratumoral distribution of fluorine-18-fluorodeoxyglucose *in vivo*: high accumulation in macrophages and granulation tissues studied by microautoradiography.

- J Nucl Med* 1992; 33: 1972–1980.
18. Wyss MT, Weber B, Honer M, Späth N, Ametaney SM, Westera G, et al. ^{18}F -choline in experimental soft tissue infection assessed with autoradiography and high-resolution PET. *Eur J Nucl Med Mol Imaging* 2004; 31: 312–316.
 19. Kubota R, Kubota K, Yamada S, Tada M, Takahashi T, Iwata R, et al. Methionine uptake by tumor tissue: a microautoradiographic comparison with FDG. *J Nucl Med* 1995; 36: 484–492.
 20. Zeisel SH. Dietary choline: biochemistry, physiology, and pharmacology. *Annu Rev Nutri* 1981; 1: 95–121.
 21. Roivainen A, Forsback S, Groenroos T, Lehtikoinen P, Kaehkoenen M, Sutinen E, et al. Blood metabolism of [methyl- ^{11}C]choline; implications for *in vivo* imaging with positron emission tomography. *Eur J Nucl Med* 2000; 27: 25–32.
 22. Pieterman RM, Que TH, Elsinga PH, Pruim J, van Putten JWG, Willemsen ATM, et al. Comparison of ^{11}C -choline and staging of patients with thoracic cancer. *J Nucl Med* 2002; 43: 167–172.